9-1-2021

Carbon dioxide uptakes by acetylene by-products through gas–solid and gas–solid–liquid reactions

Maisa El Gamal
Zayed University, maisa.elgamal@zu.ac.ae

Ameera Mohammad
United Arab Emirates University; KU Leuven

Suhaib Hameedi
Zayed University

Hadeel AlZawahreh
Zayed University

Available online at www.sciencedirect.com
ScienceDirect
Energy Reports 7 (2021) 193–198
www.elsevier.com/locate/egyr

6th International Conference on Advances on Clean Energy Research, ICACER 2021 April 15–17, 2021, Barcelona, Spain

Carbon dioxide uptakes by acetylene by-products through gas–solid and gas–solid–liquid reactions

Maisa El Gamal[a,*], Ameera Mohammad[b,c], Suhaib Hameedi[a], Hadeel AlZawahreh[a]

[a] College of Natural and Health Sciences, Zayed University, Abu Dhabi, United Arab Emirates
[b] College of Engineering, UAE University, Al Ain, United Arab Emirates
[c] Chemical Engineering Department, KU Leuven, Leuven, Belgium

Received 19 May 2021; accepted 9 June 2021

Abstract

In this work, carbon dioxide uptake value by acetylene by-products was evaluated through two types of carbonation reactions. In the first reaction, solid acetylene by-products were reacted with a simulated effluent CO_2 gas (10% CO_2 and 90% air) and the maximum uptake value of carbon dioxide per unit mass of reacted solids was calculated. In the second reaction, the mixed solid acetylene by-product with distilled water at a specific mass to volume ratio was reacted with the same effluent CO_2 gas to compare the maximum CO_2 uptake value with the first reaction. It was found that a superior CO_2 uptake in the case of G-S-L reaction with a value of 0.34 g CO_2/g *ABP* over that found in the case of G-S system of 0.14 g CO_2/g *ABP*. The fresh (unreacted) and treated acetylene by-products from both reactions were analyzed to study the effect of carbonation process on solids morphology, average particle size and carbon content. The structural and chemical characteristics of the fresh and carbonated acetylene by-products were investigated using X-ray diffraction, scanning electron microscopy and thermogravimetric analysis. The fresh acetylene by-products showed a major structure of portlandite crystals. All carbonated products exhibited a calcite crystal structure but with different morphology and particle size for each specific chemical reaction.

Peer-review under responsibility of the scientific committee of the 6th International Conference on Advances on Clean Energy Research, ICACER, 2021.

Keywords: Acetylene by-products; Carbonation; CO_2 uptake value; Solid waste; Waste utilization

1. Introduction

Previously, industrial wastes were considered to be a problem and load on the manufacturing economy [1]. New investigations prove that these wastes could be successfully utilized in new chemical reactions and have a positive industrial or environmental impact [2,3]. As an example, alkaline wastes have a significant feature of high pH value which makes them an excellent choice for CO_2 sequestration processes [4,5]. Dual beneficial could be achieved; the first is decreasing the impact of greenhouse gasses and the second is the neutralization of the unstable and high

* Corresponding author.
E-mail address: maisa.elgamal@zu.ac.ae (M. El Gamal).

https://doi.org/10.1016/j.egyr.2021.06.033

Peer-review under responsibility of the scientific committee of the 6th International Conference on Advances on Clean Energy Research, ICACER, 2021.

Nomenclature

ABP	Acetylene by-product
G-S	Gas and solid carbonation system
V_{un}	The volume of unreacted CO_2 gas (L)
V_{total}	The total volume of CO_2 fed to the system (L)
F	Gas flow rate (L/min)
t	Total time of carbonation (min)
$CO_2\%_{\text{in feed gas}}$	Volumetric % of CO_2 in the feed gas
MW_{CO_2}	CO_2 molecular weight (g/mol)
DW	Distilled water
G-S-L	Gas, Solid and liquid carbonation system
V_{react}	The volume of reacted CO_2 (L)
$CO_2\%$	CO_2 reading by the gas analyzer
dt	Time increment (min)
Upt_{CO_2}	The uptake value of CO_2 gas (gCO_2/g APB)
V_{Mol}	CO_2 gas molar volume (L/mol)
ABP_{mass}	Acetylene by-product mass (g)

reactivity solid wastes into more stable and useful products. Recently, industrial wastes such as phosphor–gypsum, steel slag/dust, and fly ash have been examined for CO_2 sequestration. Though, special pretreatment such as thermal activation and acid dissolution may be required due to the low reactivity of such waste materials [5,6].

Acetylene synthesis by-product, which is also known as lime sludge, are produced by hydrolysis reactions of calcium carbide (CaC_2) on the form of aqueous slurry [7]. The collected by-products are mainly consisting of calcium hydroxide (strong alkaline) with a mass percentage around 85% [5]. Accordingly, the utilization of these products in the CO_2 sequestration process considered to be a promising and sustainable alternative of the synthesized CO_2 adsorbent and sorbent materials. In this work, the reaction of acetylene by-products *(ABP)* with CO_2 gas will be carried out based on the gas–solid (G-S) or gas–solid–liquid reactions, to determine the maximum CO_2 uptake value based on the adsorption and absorption reactions, where the (G-S-L) reaction phase may play a significant role in determining the extreme CO_2 uptake value.

2. Methodology

2.1. Acetylene by-product (ABP) samples

Samples of acetylene by-product were collected from Arabian Industrial Gases Co., Ras Al-Khaimah, UAE. The samples were first dried at 105 °C for 6 h, next, the samples were grinded to have fine particles (∼90 μm). The samples were then characterized and used in the experiments.

2.2. Experimental procedure and setup

The schematic diagram of the carbonation process and systems setup is illustrated in Fig. 1. For the G-S-L reaction, Fig. 1(a), a plexiglass vessel in which the solid samples and distilled water mixture was exposed to a continuous flow of the gas. For the G-S reaction, Fig. 1(b), a plexiglass reactor with a distributor plate from the bottom enable the gas to interact with solid sample particles loaded initially inside the reactor system. The gas used in both reactions is a carbon dioxide with air gas mixture (10% CO_2 and balance volume is air), and the gas flow rate was controlled by mass flow controller unit. The output gas stream from both systems were directed to a CO_2 gas analyzer (Model 600 Series-Nondispersive infrared). The treated solid samples were then collected after each reaction, dried, grinded and then characterized as done to the feed samples using X-ray diffraction (*XRD*), Thermogravimetric analysis (*TGA*) and scanning electron microscopy (*SEM*). In the G-S-L system, the plexiglass

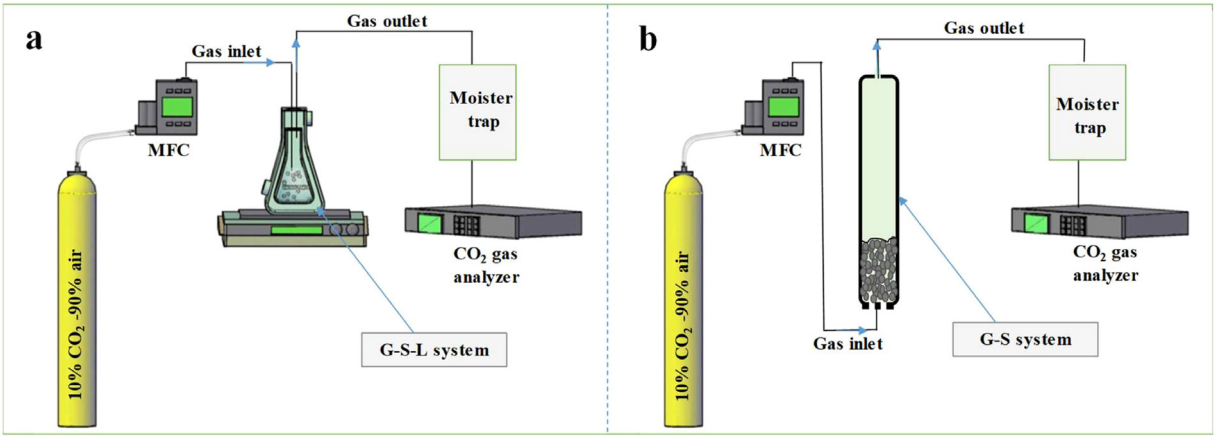

Fig. 1. A schematic diagram for the (a) G-S-L system; (b) G-S system.

vessel was filled with constant solid to liquid ratio mixture of the solid sample and distilled water (40 g ABP: 400 ml DW), while in the G-S system, the plexiglass reactor was filled only with solid sample of acetylene by-product with a mass of 40 g ABP.

For both systems (G-S & G-S-L), the chemical reactions were carried out at room temperature (23 °C) and atmospheric pressure (1 atm). The pH level was measured before and after the carbonation process. The CO_2-air gas mixture flow rate was controlled to be 1.0 L/min. The CO_2 uptake value with time was recorded by integrating the function of CO_2 capture with the carbonation reaction time, as explained in the next section, until the state of full saturation is reached (CO_2 capturing of 0%). After full saturation with CO_2 gas for both systems, the treated solid samples were collected and dried at 105 °C for 6 h to be ready for the analysis

2.3. CO_2 uptake value calculation

The CO_2 gas analyzer provides readings in volume percentages which could be converted to equivalent value in term of CO_2 uptake. The uptake value represents the mass of CO_2 that has been consumed over the mass of *ABP* used in each system (mass of CO_2 sequestered in g/mass of *ABP* in g). Accordingly, to find the uptake value for each system the following calculations are followed [4,8]. First, to calculate the unreacted CO_2 volume, Eq. (1) is used:

$$V_{un} = F \int_0^t \frac{CO_2\%}{100} dt \tag{1}$$

Then, the total volume of CO_2 which was fed to the system is calculated according to Eq. (2)

$$V_{total} = F \times \frac{CO_2\%in\ feed\ gas}{100} \times t \tag{2}$$

To calculate the sequestrated CO_2 by ABP in each system, following equation is used:

$$(V_{react}) = V_{total} - V_{un} \tag{3}$$

The volume of CO_2 sequestrated is then converted to mass through molar volume relationship and divided by the mass of *ABP* to have the CO_2 uptake value according to the following equation:

$$Upt_{CO_2}\,(gCO_2/gABP) = \left(\frac{V_{react}}{V_{Mol}} \times MW_{CO_2}\right) \div ABP_{mass} \tag{4}$$

3. Results and discussion

3.1. Carbon dioxide uptakes via gas–solid–liquid and gas–solid systems

In the G-S-L system, the introduced CO_2 gas will react with the alkaline metal content of the *ABP* in the soluble ionized carbon dioxide form ($HCO_3^{-1}{}_{(aq)}$ and $CO_3^{-2}{}_{(aq)}$) and insoluble gaseous form ($CO_{2\ (g)}$) [9]. On the other hand,

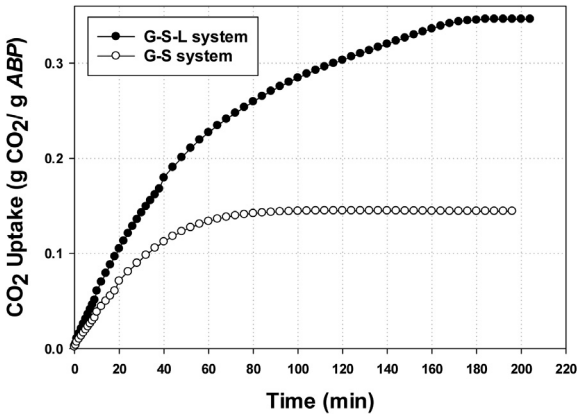

Fig. 2. CO_2 uptake values for G-S-L and G-S system with time.

in the G-S system, the insoluble gaseous form of carbonate dioxide is the only form of CO_2 in the reaction media. Consequently, CO_2 with its different forms reacts with the active alkali metal oxide and hydroxide in the G-S-L and G-S system. It is worth to mention that in the G-S-L system; more calcium hydroxide form is available due to the presence of water which converts a part of the metal oxide to a metal hydroxide form. The high initial alkalinity of *ABP* solids promotes the CO_2 sequestration due to the acidic nature of CO_2 molecules, and during reaction, the pH value will be gradually decrease until full saturation with CO_2 molecules will be reached and no more sequestration is observed. The experimental CO_2 uptake value was then calculated according to Eqs. (1)–(4) and found to reach 0.34 g CO_2/g *ABP* for the G-S-L system and 0.14 g CO_2/g *ABP* for the G-S system, as shown in Fig. 2. It is clear that the maximum CO_2 uptake value could be reached in the G-S-L system and this can be explained and related to the effect of liquid phase in improving the diffusion of CO_2 inside the reaction media. Additionally, higher mass transfer and low diffusion resistance are contributed to the presence of different forms of the reactive carbon dioxide molecule and metal reactive components compared to the only gaseous form of CO_2 in the G-S system [10].

3.2. Fresh and reacted ABP solid characteristics

The chemical composition of fresh *ABP* sample was determined using inductively coupled plasma (ICP-AES); it was found that CaO content to be around 86% and MgO, FeO, Al_2O_3, and SiO_2 to be around 0.17%, 0.06%, 1.3%, and 2.5%, respectively. The solid samples were also characterized using X-ray powder diffraction (*XRD*) and showed that it mainly comprised Portlandite with unreacted carbon in the form of graphite [11]. Thermogravimetric analysis (*TGA*) showed three thermal degradation temperature ranges of 150 °C, 400–620 °C, and 620–900 °C, which corresponded to the removal of water, Portlandite decomposition [12], and release of carbon dioxide, respectively. The external morphology of fresh ABP samples as examined by scanning electron microscopy (*SEM*), Fig. 3, shows that *APB* particles are aggregates of small, irregularly stacked calcium oxide and hydroxide crystals [13].

The *XRD* analysis for the carbonated *ABP* samples from both systems exhibited calcite crystal structures [14] compared to the portlandite crystal in the fresh *ABP*, as shown in Fig. 4. The analysis confirms that the carbonation system is only affected the morphology and size distribution of the calcite crystals. This was indicated by the minor changes in the peak intensity at each operated system [15]. The *SEM* analysis for the carbonated *ABP* samples by the G-S-L system showed a mixture of singular elongated rods and agglomerated spheroidal particles [16] with an average size of 0.32–2.08 μm as shown in Fig. 5(a), while the carbonated solids by the G-S system showed a calcite particle size of 0.59–1.34 with scalenohedral morphology and no spheroidal particles as indicated by Fig. 5(b).

4. Conclusions

Carbon dioxide uptakes by high alkalinity acetylene by-products (ABP) in a gas–solid and gas–solid–liquid reaction systems have been examined. The same operating conditions of ABP mass, carbon dioxide-air mixture composition and flow rate were conducted in two different reactor systems, (Gas–Solid) and (Gas–Solid–Liquid),

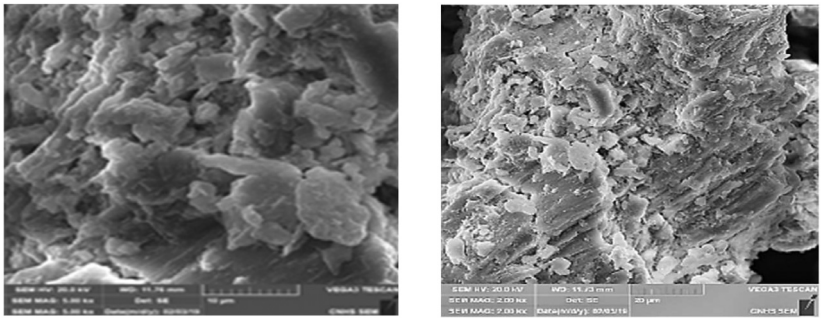

Fig. 3. *SEM* images showing the morphology of the ABP fresh solid particles.

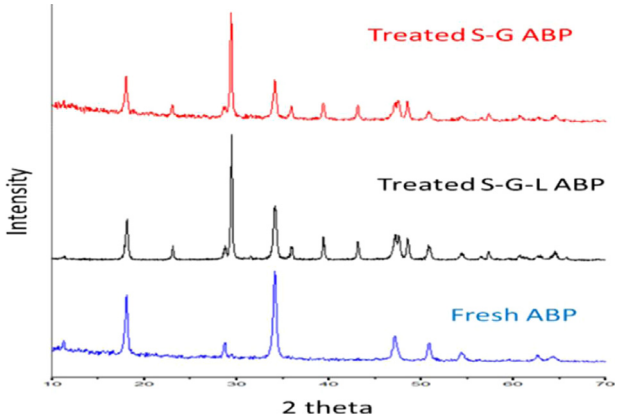

Fig. 4. X-ray diffraction graphs of carbonated ABP samples at G-S-L and G-S systems over 2θ = 5°–70°.

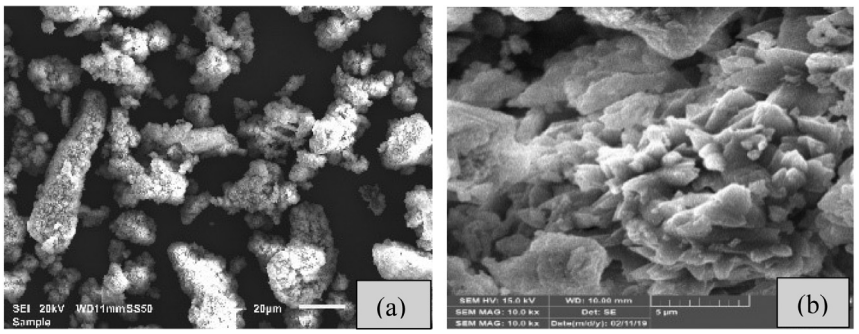

Fig. 5. *SEM* images showing the morphology of the carbonated ABP in the (a) G-S-L and (b) G-S systems.

to detect the change of CO_2 uptake with time. The fresh acetylene by-products showed portlandite crystals while the reacted ones showed the calcite crystals. Different morphology and particles size were observed for each reaction; in the (G-S) system, a calcite particle with scalenohedral morphology was observed, while in the (G-S-L), a mixture of singular elongated rods and agglomerated spheroidal particles were detected. A maximum CO_2 uptake value for the gas–solid–liquid reaction of 0.34 g CO_2/g *ABP* was recorded and explained by the higher diffusion, mass transfer and ions concentration, and 0.14 g CO_2/g ABP of G-S system. Additional examination regards the effect of carbonation conditions such as different gas flow rates, temperatures and initial pH are still essential to have full evaluation of the carbon dioxide uptakes for the two-proposed system (G-S & G-S-L). The focus of the future work will be to carry out a full statistical analysis to optimize each system for high carbon dioxide uptakes.

Declaration of competing interest

The authors declare that they have no known competing financial interests or personal relationships that could have appeared to influence the work reported in this paper.

Acknowledgments

The authors would like to acknowledge the financial support of the Research Office at Zayed University (United Arab Emirates, Abu Dhabi) RIF grant code R19050. Our special thanks are extended to the Arabian industrial gases company (Gulf Cryo) for their cooperation and for providing samples.

References

[1] Mbuligwe SE, Kaseva ME. Assessment of industrial solid waste management and resource recovery practices in Tanzania. Resour Conserv Recy 2006;47(3):260–76.
[2] Sun J, Geng CL, Zhang ZT, Wang XT, Xu L. Present situation of comprehensive utilization technology of industrial solid waste. Mater Rev 2012;11(2):105–9.
[3] El Gamal M, Mohamed AMO, Hameedi S. Stabilization of active acetylene by-product via sequestration of CO_2. In: Wastes: solutions, treatments and opportunities III: selected papers from the 5th international conference wastes 2019. Lisbon, Portugal: CRC Press; 2019, p. 149.
[4] Ibrahim MH, El-Naas MH, Zevenhoven R, Al-Sobhi SA. Enhanced CO_2 capture through reaction with steel-making dust in high salinity water. Int J Greenh Gas Control 2019;91:102819.
[5] El Gamal M, Mohamed A-M, Hameedi S. Treatment of industrial alkaline solid wastes using carbon dioxide. In: Sustainable development and social responsibility, vol. 1. Springer; 2020, p. 317–23.
[6] Mohamed AMO, El-Gamal M, Hameedi S. Advanced mineral carbonation: An approach to accelerate CO_2 sequestration using steel production wastes and integrated fluidized bed reactor. In: International symposium on energy geotechnics. Cham: Springer; 2018, p. 387–93.
[7] Schobert H. Production of acetylene and acetylene-based chemicals from coal. Chem Rev 2014;114(3):1743–60.
[8] Ameera F. Mohammad MHE-N, Suleiman Mabruk I, Al Musharfy Mohamed. Optimization of a Solvay-based approach for CO_2 capture. Int J Chem Eng Appl 2016;7(4):230–4.
[9] Olivo A, Ghedini E, Signoretto M, Compagnoni M, Rossetti I, vs Liquid. Liquid vs gas phase CO_2 photoreduction process: which is the effect of the reaction medium? Energies 2017;10(9):1394.
[10] Kucka L, Kenig EY, Górak A. Kinetics of the gas-liquid reaction between carbon dioxide and hydroxide ions. Ind Eng Chem Res 2002;41(24):5952–7.
[11] Badenhorst CJ, Wagner NJ, Valentim BRV, Santos AC, Guedes A, Białecka B, Całus J, Popescu LG, Cruceru M, Predeanu G. Char from coal ash as a possible precursor for synthetic graphite–Recent developments of the Charphite project. In: Proceedings of the world of coal ash (WOCA); 2019. p. 13–6.
[12] Villagrán-Zaccardi YA, Egüez-Alava H, De Buysser K, Gruyaert E, De Belie N. Calibrated quantitative thermogravimetric analysis for the determination of portlandite and calcite content in hydrated cementitious systems. Mater Struct 2017;50(3):1–10.
[13] Stankic S, Bernardi J, Diwald O, Knözinger E. Optical surface properties and morphology of MgO and CaO nanocrystals. J Phys Chem B 2006;110(28):13866–71.
[14] Kontoyannis CG, Vagenas NV. Calcium carbonate phase analysis using XRD and FT-Raman spectroscopy. Analyst 2000;125(2):251–5.
[15] Gómez DA, Coello J, Maspoch S. The influence of particle size on the intensity and reproducibility of Raman spectra of compacted samples. Vib Spectrosc 2019;100:48–56.
[16] Shahwan T, Zünbül B, Tunusoğlu Ö, Eroğlu AE. AAS, XRPD, SEM/EDS, and FTIR characterization of Zn2+ retention by calcite, calcite–kaolinite, and calcite–clinoptilolite minerals. J Colloid Interface Sci 2005;286(2):471–8.